International Journal of Cardiology 293 (2019) 203–210

Contents lists available at ScienceDirect

International Journal of Cardiology

journal homepage: www.elsevier.com/locate/ijcard

Effects of combined angiotensin II receptor antagonism and neprilysin inhibition in experimental pulmonary hypertension and right ventricular failure

Stine Andersen [a,*,1], Julie Birkmose Axelsen [a,1], Steffen Ringgaard [b,1], Jens Randel Nyengaard [c,1], Janus Adler Hyldebrandt [d,1], Harm Jan Bogaard [e,1], Frances S. de Man [e,1], Jens Erik Nielsen-Kudsk [a,1], Asger Andersen [a,1]

[a] Department of Cardiology, Aarhus University Hospital, Denmark
[b] MR Centre, Aarhus University Hospital, Denmark
[c] Core Center for Molecular Morphology, Section for Stereology and Microscopy, Department of Clinical Medicine, Centre for Stochastic Geometry and Advanced Bioimaging, Aarhus University, Denmark
[d] Department of Anesthesiology and Intensive Care, Aarhus University Hospital, Denmark
[e] Department of Pulmonology, Amsterdam UMC, the Netherlands

ARTICLE INFO

Article history:
Received 18 February 2019
Received in revised form 3 June 2019
Accepted 24 June 2019
Available online 29 June 2019

Keywords:
Pulmonary hypertension
Natriuretic peptides
Angiotensin II
Animal models
Right ventricular failure

ABSTRACT

Background: Combined angiotensin II receptor antagonism and neprilysin inhibition by LCZ696 reduces morbidity and mortality in heart failure patients and works by reducing RAAS activity and increasing cGMP levels. This study aims to evaluate the effects of LCZ696 in rats with pulmonary hypertension and right ventricular (RV) failure.
Methods: Pulmonary hypertension was induced in rats ($n = 34$) by combined exposure to the vascular endothelial growth factor-receptor antagonist SU5416 and hypoxia (SuHx). To distinguish pulmonary vascular from cardiac effects, isolated RV failure was induced by pulmonary trunk banding (PTB) in another group of rats ($n = 40$). In both models, the development of RV dysfunction was verified before randomization to treatment with LCZ696 (60 mg/kg/day) or vehicle for five weeks.
Results: In the SuHx rats, LCZ696 treatment reduced the increase in RV pressure and the development of RV hypertrophy and RV dilatation compared with vehicle treatment. LCZ696 also reduced wall thickness of the smaller pulmonary arteries. In the PTB rats, LCZ696 treatment did not have any effects on RV hypertrophy or function.
Conclusions: Combined angiotensin II receptor antagonism and neprilysin inhibition reduced RV systolic pressure, hypertrophy, and dilatation in rats with pulmonary hypertension. These effects seem secondary to pulmonary vascular changes, including reduced pulmonary vascular remodeling, as similar effects were not seen in rats with isolated RV failure. LCZ696 may have a therapeutic potential in the treatment of pulmonary hypertension.

1. Introduction

In pulmonary arterial hypertension (PAH), remodeling of the smaller pulmonary arteries causes an increase in pulmonary vascular resistance and thereby an increase in afterload of the right ventricle (RV). Initially, the RV adapts to the pressure overload by hypertrophy and increased contractility, but with disease progression, these adaptations are no longer sufficient to maintain cardiac output and the RV fails. Neurohormonal activation plays a central role in PAH and the concomitant development of RV failure. Up-regulation of the renin-angiotensin-aldosterone-system (RAAS) contributes to pulmonary vascular remodeling [1], and in idiopathic PAH patients, systemic RAAS activity is associated with disease progression and the risk of death or lung transplantation [2].

Contrary to the RAAS, activation of the natriuretic peptide system exerts cardioprotective effects. Atrial natriuretic peptide (ANP) and brain natriuretic peptide (BNP) are released from the overloaded heart and promote vasodilatation, reduce fibrosis, and suppress the RAAS and sympathetic nervous system overdrive. The peptides are, however, quickly degraded by the enzyme neprilysin. The natriuretic peptides have antiproliferative effects on pulmonary vascular smooth muscle cells [3,4], and ANP and BNP vasorelaxation is crucial in attenuating the development of hypoxia induced PH [5]. In the clinical setting, infusion with the recombinant human BNP nesiritide reduces pulmonary vascular resistance in postcapillary pulmonary hypertension (PH) [6,7]. In precapillary PH, nesiritide infusion increases nitric oxide levels

* Corresponding author at: Department of Cardiology, Aarhus University Hospital, Palle Juul-Jensens Boulevard 99, 8200 Aarhus N, Denmark.
E-mail address: stineandersen@clin.au.dk (S. Andersen).
[1] This author takes responsibility for all aspects of the reliability and freedom from bias of the data presented and their discussed interpretation.

https://doi.org/10.1016/j.ijcard.2019.06.065
0167-5273/

[7] and augments the pulmonary vasodilating effects of sildenafil [8], but the effects of long-term stimulation of the natriuretic peptide system have not yet been evaluated in PH patients.

LCZ696 attenuates the harmful effects of the RAAS while enhancing the beneficial effects of the natriuretic peptides by combining the angiotensin II receptor antagonist valsartan and the neprilysin inhibitor sacubitril. The compound reduces morbidity and mortality in patients with left ventricular failure [9], but no data exist regarding its effect on PH and the pressure overloaded RV.

This study was designed to evaluate the effects of combined angiotensin II receptor antagonism and neprilysin inhibition by LCZ696 in experimental PH and RV failure and to distinguish pulmonary vascular effects from potential direct cardiac effects by using two animal models; one of PH with RV failure and one of isolated RV failure.

2. Methods

2.1. Study design (Fig. 1)

Effects of LCZ696 treatment on the development of PH and RV failure was evaluated in the Sugen-hypoxia (SuHx) model. Sprague-Dawley rats (177 ± 19 g) were randomized to sham or PH and RV failure by SuHx as previously described [10]. In order to separate pulmonary vascular effects of LCZ696 treatment from direct cardiac effects, we included another group of rats with isolated RV failure. For this part of the study, Wistar rat weanlings (123 ± 11 g) were randomized to sham, compensated RV failure, or decompensated RV failure by pulmonary trunk banding (PTB) as previously described [11]. Details on the animal models are provided in the supplementary material.

All rats received humane care and were treated according to Danish national guidelines. All experiments were approved by the Institutional Ethics Review Board and conducted in accordance with the Danish law for animal research (authorization numbers 2016-15-0201-00936 and 2016-15-0201-01040, Danish Ministry of Justice).

2.2. Hemodynamic measurements

Hemodynamics were evaluated by echocardiography, cardiac MRI, and invasive pressure and volume measurements before euthanasia. For details, see supplementary. In short, we used a Vevo 2100 echocardiographic system (Visual Sonics, Canada) at baseline and end of study to obtain measures of RV function including tricuspid annular plane systolic excursion (TAPSE). A 9.4 Tesla Agilent magnetic resonance imaging (MRI) system was used for assessment of RV volumes. RV stroke volume was assessed from phase contrast flow measurements in the pulmonary artery. PTB-decomp rats did not undergo MRI or pressure-volume loop recordings, as the severity of their disease did not allow for longer periods of anesthesia. Systemic blood pressure and RV pressure and volume were measured invasively with micro-tip catheters (SPR-869; Millar Instruments, USA). Pressure-volume loops with decreasing preloads were generated by slow occlusion of the inferior cava. Data were recorded and analyzed using LabChart (AD Instruments, UK). All data analyses were performed by a blinded observer.

2.3. Stereology

Stereological methods and principles were used for evaluation of morphological changes of the pulmonary vasculature and RV tissue. For details, see supplementary. All analyses were performed with the observer blinded to the source of the sample.

In short, isotropic 2 μm paraffin sections of lung tissue from SuHx and corresponding sham rats were made using the orientator technique [12]. Sections were stained with elastica van Gieson and analyzed using Visiopharm software (Hørsholm, Denmark). Pulmonary arteries with an outer diameter < 90 μm and sampled by an unbiased counting frame were included in the analysis. Vessels were classified into three groups according to their outer diameter [10]. Outer and inner diameter of the vessels were measured in the short axis and wall thickness calculated as:

$$Wall\ thickness\ (\mu m) = \frac{Outer\ diameter\ (\mu m) - Inner\ diameter\ (\mu m)}{2}$$

Thin isotropic cryosections were prepared from the RV by the isector technique [13] after sampling by the smooth fractionator principle. To estimate fibrosis, sections were stained with Masson's trichrome and analyzed using two point grids; a 12 × 12 point grid for fibrosis and 3 × 3 point grid for the RV. Volume fraction, V_V, of fibrosis was calculated for each animal by the formula:

$$V_V(fib/RV) = \frac{\Sigma P(fib)}{\Sigma P(RV)} \cdot \frac{9}{144}$$

Reference volume of the RV was estimated by dividing the wet weight of the RV by 1.06 (g/cm^3) [14] and total fibrosis volume, $V(fib)$, calculated as

$$V(fib, RV) = V_V(fib/RV) \cdot V(RV)$$

To estimate capillary length density and total length, isotropic cryosections were prepared with immunohistochemical staining for the endothelial marker CD31. Capillaries were sampled by an unbiased counting frame, and capillary length density, $Lv(cap/RV)$, i.e. number of capillary profiles per RV area was calculated as

$$Lv(cap/RV) = \frac{2 \cdot Q_A(cap)}{a/p \cdot \Sigma P(RV)},$$

where a/p, is the area per point of the RV point grid, and $Q_A(cap)$ is the number of capillary profiles.

Total length, $L(cap,RV)$, was calculated as:

$$L(cap, RV) = Lv(cap/RV) \cdot V(RV)$$

The diffusion length (r) i.e. the radius of the cross-sectional area of the tissue around a capillary supplied by that capillary, assuming that each capillary has a cylindrical shape and supplies a tissue cylinder, was calculated as

$$r = \sqrt{\frac{1}{\pi \cdot Lv(cap/RV)}}$$

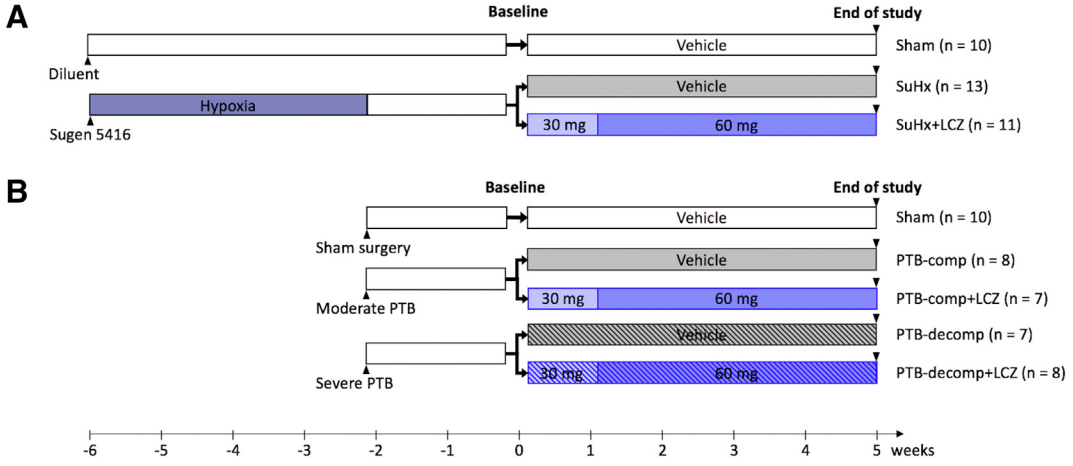

Fig. 1. Study design. The SuHx model was used to evaluate the effects of LCZ696 treatment in rats with PH and RV failure (A). After four weeks in hypoxia, an echocardiography verified the development of PH by RV dilatation in the SuHx rats, and they were returned to normoxia. After additional two weeks, a baseline echocardiography was performed in all rats to evaluate RV function, and the SuHx rats were randomized to vehicle (SuHx) or LCZ696 treatment (SuHx+LCZ) by once daily oral gavage. For up-titration, the treatment group received a low dose of LCZ696 (30 mg/kg/day) for the first week followed by full dose (60 mg/kg/day) for four weeks. The PTB model was used to evaluate the potential direct cardiac effects of LCZ696 in both compensated and decompensated RV failure (B). Two weeks after the procedure, an echocardiography was performed to verify RV dysfunction in PTB rats, and they were randomized to vehicle (PTB-comp, PTB-decomp) or LCZ696 treatment (PTB-comp+LCZ, PTB-decomp+LCZ) administered as described above. Sham rats (Sham) from both models received vehicle treatment. See supplementary for methodological details on the SuHx and PTB models.

2.4. Gene expression

After sampling for stereology, remaining RV tissue blocks were frozen (−80 °C) for evaluation of mRNA expression levels of: ANP, BNP, α-myosin heavy chain (α-MHC), β-myosin heavy chain (β-MHC), α-smooth muscle actin (α-SMA), connective tissue growth factor (CTGF), osteopontin (OPN), plasminogen activator inhibitor-1 (PAI-1), collagen I, and collagen III. For details, see supplementary.

2.5. Statistics

The number of rats was determined by a power calculation prior to initiation of the study (supplementary). Data were tested for normal distribution using QQ-plots. Normally distributed continuous variables are expressed as mean with 95% confidence interval (CI). Non-normal data were log-transformed and are presented as box plots. One-way analysis of variance (ANOVA) was used for evaluation of significance of differences between selected groups (SuHx and PTB vs sham and LCZ696 treatment vs vehicle), followed by post hoc Bonferroni analyses. Categorical data are presented as numbers and percentages and were compared between groups by Fisher's exact test. Comparisons of survival curves were performed by log-rank tests. Outliers were excluded from statistical analyses but presented on graphs by open dots. Intra- and inter-observer variability were evaluated for relevant key outcomes by Bland-Altman plots (supplementary material and Fig. S3). All statistical analyses were performed with the use of Graphpad Prism 6 (Graphpad Software, La Jolla, California). $p < 0.05$ was considered statistically significant.

3. Results

3.1. RV failure in the SuHx model

At baseline six weeks after SU5416 injection and two weeks after returning to normoxia, reduced cardiac index and TAPSE confirmed RV dysfunction in all SuHx rats. There was no difference between treatment groups (supplemental Table S1). Four rats died before end of study; one rat from the SuHx group and three rats from the SuHx +LCZ group with no difference in survival between the two groups ($p = 0.303$).

At end of study, RV systolic pressure and RV afterload (Ea) were increased in the SuHx rats compared with sham rats, while a corresponding increase in RV contractility (Ees) preserved ventriculo-arterial coupling (Ees/Ea). RV failure was evident by RV dilatation and reduced cardiac index the SuHx rats compared with sham rats. Furthermore, SuHx rats demonstrated RV hypertrophy and diastolic dysfunction (Eed) (Fig. 2, Table 1). mRNA expressions of the heart failure markers ANP and BNP were increased in the SuHx rats, while reduced α-MHC expression and increased β-MHC expression confirmed α- to β-isotype switch characteristic of maladaptive cardiac growth (supplemental Fig. S4).

3.2. Reduced RV pressure, hypertrophy, and dilatation

Treatment with LCZ696 reduced RV systolic pressure and RV hypertrophy compared with vehicle treatment. Furthermore, rats treated with LCZ696 had less RV dilatation with lower RV end-diastolic and end-systolic volumes compared with vehicle treated SuHx rats. RV ejection fraction and RV stroke volume were unaltered. Compared with vehicle, LCZ696 did not have any effects on RV contractility or diastolic function, nor did it improve cardiac index (Fig. 2, Table 1). LCZ696 reduced mean arterial blood pressure by approximately 12% compared with vehicle (Table 1).

3.3. Pulmonary vascular remodeling

Combined exposure to SU5416 and hypoxia induced remodeling of the pulmonary vasculature evident by increased wall thickness of the smaller pulmonary arteries (PA wall thickness). Treatment with LCZ696 reduced wall thickness of arteries with an outer diameter between 30 and 60 μm. There was a trend towards reduced remodeling in arteries with an outer diameter between 60 and 90 μm ($p = 0.08$) (Fig. 2). There was no difference in tissue shrinkage between the groups.

3.4. Compensated and decompensated RV failure in the PTB model

Two weeks after surgery, RV dysfunction was confirmed in all PTB rats by echocardiography. There was no difference between treatment groups (supplemental Table S2). Amongst the PTB rats with compensated RV failure, one rat (from the PTB-comp+LCZ group) died before end of study. Amongst the PTB rats with decompensated RV failure, four rats died before end of study (two PTB-decomp and two PTB-decomp+LCZ rats). At end of study, RV systolic pressure was increased in both the compensated and the decompensated PTB rats compared with sham. TAPSE was reduced in compensated PTB rats compared with sham and in decompensated PTB rats compared with both compensated PTB rats and sham rats. There was a similar stepwise decrease in cardiac index (Table 1, Fig. 2). The decompensated stage of RV failure was confirmed by extracardiac manifestations of heart failure including liver congestion and fluid retention (hydrothorax and ascites), which were present in 86% and 88% of the PTB-decomp rats compared with 25% and 0% in the PTB-comp rats ($p < 0.05$ and $p < 0.01$) (supplemental Table S4). Heart failure was confirmed in the PTB rats by increased mRNA expression levels of ANP, BNP, and β-MHC and decreased α-MHC compared with sham rat levels. There were no differences between compensated and decompensated PTB rats (supplemental Fig. S5).

3.5. No hemodynamic effects of LCZ696 in the PTB model

In the PTB model of isolated RV failure, treatment with LCZ696 reduced systemic blood pressure but not RV systolic pressure in rats with compensated RV failure and in rats with decompensated RV failure. Likewise, there were no effects on RV hypertrophy, RV dilatation, or RV function in the rats treated with LCZ696 compared with vehicle treated rats (Fig. 2, Table 1).

3.6. RV remodeling

There was a 4-fold increase in the volume fraction of fibrosis in the RV in both the SuHx and the PTB rats compared with the corresponding sham groups. With the higher RV volume of the SuHx and PTB rats, this corresponded to a 10-fold increase in the total volume of fibrosis (Fig. 3). Likewise, the mRNA expressions of the profibrotic proteins CTGF, OPN, and PAI-1 and the myofibroblast marker α-SMA were increased in the SuHx and PTB rats compared with sham rats. mRNA expressions of collagen I and collagen III were increased in the PTB but not in the SuHx rats compared with sham (supplemental Fig. S4 and S5). Treatment with LCZ696 did not affect the development of fibrosis in the SuHx or in the PTB model.

Pressure overload induced RV hypertrophy was accompanied by angiogenesis evident by an increase in total capillary length in both SuHx and PTB rats compared with sham rats. The angiogenic response was, however, not sufficient to prevent a decrease in capillary length density, i.e. the number of capillaries per RV area, or diffusion length (Fig. 3).

4. Discussion

This study investigated the effects of combined angiotensin II receptor and neprilysin inhibition by LCZ696 in two different animal models; one of PH and RV failure and one of isolated RV failure. Using advanced imaging techniques, pressure-volume analyses, and stereology, we demonstrate that:

1) In SuHx rats with PH and RV failure, treatment with LCZ696 reduced RV systolic pressure, RV hypertrophy, and RV dilatation.
2) These effects are caused, at least partly, by a reduction in pulmonary vascular remodeling.
3) In the PTB model of isolated RV failure, LCZ696 did not have any effects on RV function or remodeling, indicating that the beneficial effects seen in the SuHx model are caused by pulmonary vascular changes rather than direct cardiac effects.

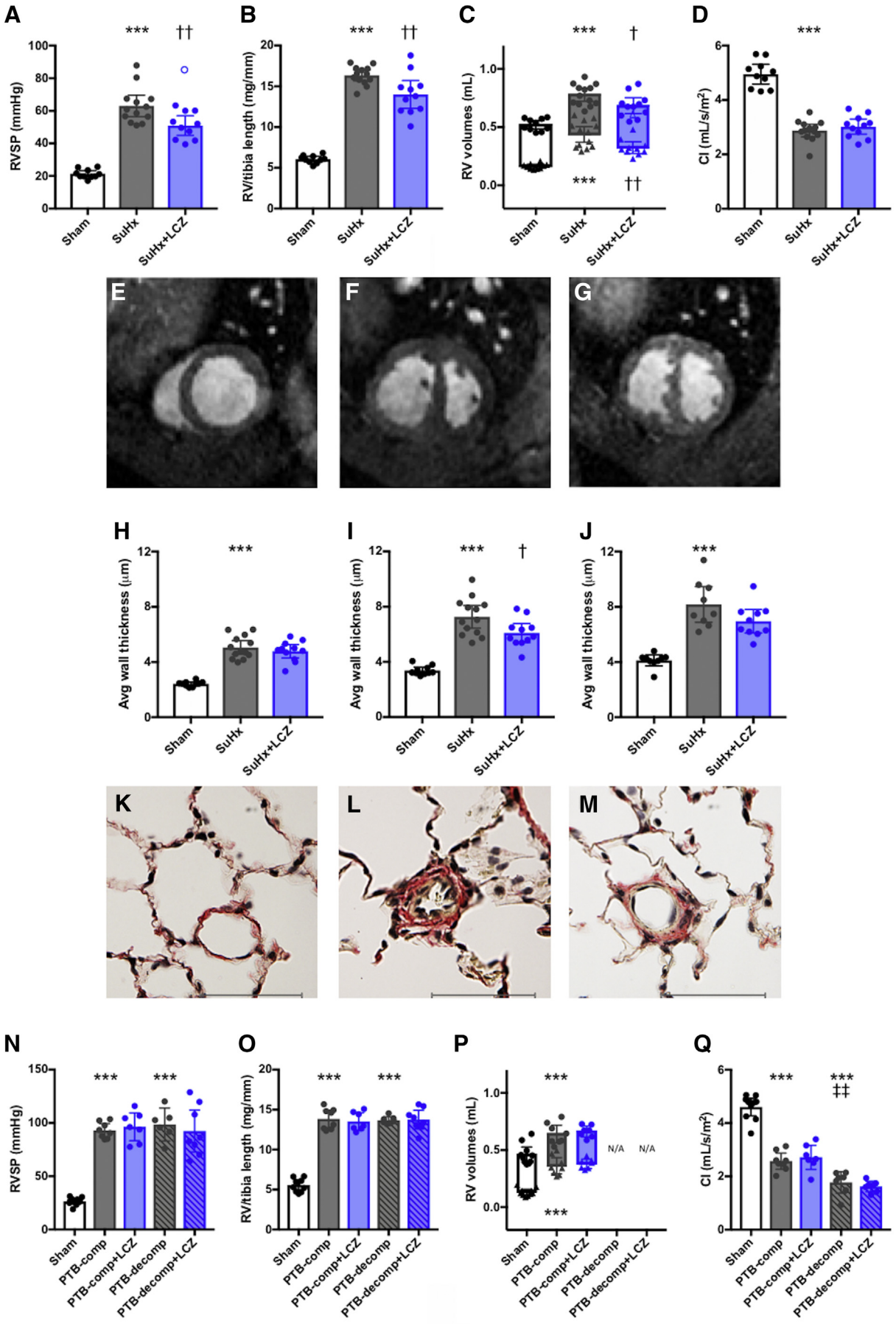
A
RVSP (mmHg)
Sham
SuHx
SuHx+LCZ
B
RV/tibia length (mg/mm)
C
RV volumes (mL)
D
CI (mL/s/m²)
E
F
G
H
Avg wall thickness (μm)
I
J
K
L
M
N
PTB-comp
PTB-comp+LCZ
PTB-decomp
PTB-decomp+LCZ
O
P
N/A
Q

Table 1
Data at end of study.

	SuHx model			PTB model				
	Sham ($n = 10$)	SuHx ($n = 13$)	SuHx + LCZ ($n = 11$)	Sham ($n = 10$)	PTB-comp ($n = 8$)	PTB-comp + LCZ ($n = 7$)	PTB-decomp (n = 7)	PTB-decomp + LCZ ($n = 8$)
Hemodynamics								
RV EDP (mmHg)	1.6 [0.1;3.0]	6.7 [4.6;8.8]**	4.5 [1.9;7.0]	3.8 [2.5;5.1]	11.1 [8.2;14.0]**	9.8 [5.6;14.0]	7.2 [1.8;12.5]	6.5 [1.8;11.2]
RV filling pressure (mmHg)	1.7 [1.5;1.9]	3.8 [3.2;4.3]***	3.0 ± [2.6;3.4]†	2.0 [1.3;2.6]	4.1 [3.3;4.9]	3.9 [3.2;4.6]	5.0 [2.7;7.3]**	4.6 [2.2;6.9]
RV dP/dt max (mmHg/s)	1019 [915;1124]	2630 [2408;2852]***	2496 [2173;2820]	1242 [1071;1414]	3270 [2955;3586]***	3339 [2761;3918]	3891 [2964;4819]***	3434 [2888;3980]
RV dP/dt min (mmHg/s)	−870 [−974;−765]	−1947 [−2131;−1762]***	−1907 [−2159;−1655]	−1019 [−1170;−868]	−2822 [−3108;−2537]***	−2695 [−3148;−2243]	−2756 [−3169;−2343]***	−2331 [−2711;−1951]
Ees (mmHg/mL)	37 [29;45]	180 [143–218]***	166 [119;213]	55 [42;68]	240 [176;305]***	206 [155;257]	N/A	N/A
Ea (mmHg/mL)	43 [38;47]	205 [149;262]***	158 [111;206]	71 [60;83]	389 [340;438]***	430 [300;560]	N/A	N/A
Ees/Ea	0.88 [0.70;1.06]	0.91 [0.68;1.1]	0.98 [0.74;1.23]	1.12 [0.13;2.26]	0.63 [0.45;0.81]**	0.50 [0.40;0.60]	N/A	N/A
Eed (mmHg/mL)	4.4 [3.3;5.4]	8.7 [6.0;11.5]*	9.3 [5.7;12.9]	5.1 [1.9;8.4]	11.5 [8.5;14.4]*	11.6 [7.0;16.3]	N/A	N/A
PRSW (mmHg)	14 [11;17]	32 [23;40]**	30 [22;38]	12 [9;14]	36 [25;47]**	34 [18;49]	N/A	N/A
Heart rate (bpm)	319 [305;333]	289 [274;303]**	288 [276;301]	340 [315;365]	304 [285;323]	296 [277;315]	282 [256;307]***	278 [245;311]
RV EF (%)	69 [67;70]	44 [39;50]***	49 [42;56]	72 [69;74]	44 [40;49]***	43 [38;47]	N/A	N/A
TAPSE (mm)	3.3 [3.0;3.5]	2.0 [1.7;2.2]***	2.0 [1.8;2.2]	2.6 [2.3;2.9]	1.8 [1.6;1.9]***	1.7 [1.5;1.9]	1.2 [0.8;1.5]***,‡‡	1.1 [0.8;1.5]
Tricuspid regurgitation (%)	0 (0)	6 (46)*	6 (55)	0 (0)	7 (88)***	7 (100)	6 (86)***	8 (100)
Stroke volume (mL)	0.50 [0.46;0.55]	0.31 [0.26;0.37]***	0.34 [0.26;0.41]	0.45 [0.41;0.48]	0.28 [0.25;0.31]***	0.30 [0.25;0.36]	0.19 [0.16;0.23]***,‡‡	0.19 [0.16;0.22]
MAP (mmHg)	103 [96;109]	115 [0.8;122]*	103 [95;111]†	105 [95;116]	123 [113;133]*	103 [90;115]†	109 [95;123]	97 [90;105]
Anatomical data								
Body weight at end of study (g)	612 [591;633]	549 [523;575]**	520 [488;552]	409 [379;439]	411 [380;442]	407 [378;436]	379 [354;403]	387 [357;417]
RV weight (g)	0.27 [0.25;0.29]	0.73 [0.70;0.76]***	0.61 [0.54;0.69]†††	0.23 [0.20;0.25]	0.58 [0.53;0.62]	0.57 [0.52;0.62]	0.55 [0.53;0.56]	0.56 [0.51;0.61]
LV + S weight (g)	1.06 [0.99;1.12]	1.12 [1.03;1.20]	0.97 [0.87;1.06]†	0.82 [0.73;0.90]	0.96 [0.86;1.07]	0.99 [0.87;1.11]	0.75 [0.68;0.82]‡	0.83 [0.69;0.97]
RV/LV + S	0.26 [0.24;0.28]	0.66 [0.62;0.70]***	0.64 [0.57;0.72]	0.28 [0.27;0.29]	0.60 [0.55;0.65]***	0.58 [0.52;0.64]	0.73 [0.66;0.81]***,‡‡‡	0.69 [0.62;0.75]
Lungs (g)	2.12 [1.98;2.26]	2.68 [2.50;2.85]***	2.45 [2.30;2.60]	1.64 [1.49;1.80]	1.64 [1.45;1.83]	1.64 [1.50;1.78]	1.46 [1.26;1.67]	1.56 [1.37;1.75]

RV: right ventricle/ventricular; EDP: end diastolic pressure; dP/dt max: first derivative (maximal) of right ventricular systolic pressure; dP/dt min: first derivative (minimal) of right ventricular systolic pressure; Ees: end systolic elastance; Ea: arterial elastance; Eed: end diastolic elastance; PRSW: preload recruitable stroke work; EF: ejection fraction; TAPSE: tricuspid annular plane systolic excursion; MAP: mean arterial pressure; LV + S: left ventricle plus septum. Data are presented as mean [95% CI] or *n* (%).

* $p < 0.05$.
** $p < 0.01$.
*** $p < 0.001$ vs sham.
† $p < 0.05$.
††† $p < 0.001$ vs SuHx/PTB.
‡‡ $p < 0.01$.
‡‡‡ $p < 0.001$ vs PTB-comp.

Our results motivate further investigation of the role of the RAAS and the natriuretic peptides in PH and RV failure and of the therapeutic potential of combined angiotensin II receptor antagonism and neprilysin inhibition in PH patients.

4.1. Stimulation of the natriuretic peptide system and inhibition of the RAAS in experimental PH and RV failure

Continuous infusion with a neprilysin inhibitor [15] or BNP [16] attenuated the development of PH in rats during exposure to hypoxia. In this study, we demonstrate that LCZ696 was able to reverse pulmonary vascular remodeling, as we initiated treatment with LCZ696 after the SuHx rats had developed PH and returned to normoxia. In monocrotaline rats with established PH, BNP infusion decreased RV systolic pressure in the acute setting, but unlike in our study the effects of long term treatment were not tested [17].

In hypoxic rats, local lung angiotensin converting enzyme (ACE) expression was increased in the wall of newly muscularized pulmonary arteries [18], and local cardiac ACE expression was increased in the RV [19]. Continuous administration of the ACE inhibitor captopril or the angiotensin II receptor antagonist losartan reduced pulmonary vascular remodeling and RV hypertrophy in rats during 14 days exposure to

Fig. 2. Hemodynamic and pulmonary vascular effects of SuHx and PTB and of LCZ696 treatment. At end of study, increased RV systolic pressure (A) had caused hypertrophy of the RV (B) in the SuHx rats compared with sham. Treatment with LCZ696 reduced RV systolic pressure and RV hypertrophy compared with vehicle treatment. SuHx rats had increased RV end-diastolic (dots) and end-systolic (triangles) volumes, which were reduced with LCZ696 treatment (C). RV failure was evident in the SuHx rats by reduced cardiac index (D). Representative short axis MRI images of a sham rat (E), vehicle treated SuHx rat (F), and a rat treated with LCZ696 (G). Average wall thickness of the pulmonary arteries with a diameter of <30 μm (H), of 30–60 μm (I), and of 60–90 μm (J). Representative images of a normal pulmonary artery (K) and remodeled pulmonary arteries of a vehicle treated SuHx rat (L) and a SuHx rat treated with LCZ696 (M). Bar = 55 μm. At end of study seven weeks after the PTB procedure, there was a distinct increase in RV systolic pressure in PTB rats compared with sham operated rats (N). The banding also induced RV hypertrophy (O) and RV dilatation (P), which did not change with LCZ696 treatment. It was not possible to perform MRI scans for assessment of RV volumes in the PTB-decomp rats. Cardiac index (CI) decreased gradually as the severity of the banding increased, meaning that PTB rats with decompensated RV failure had an even worse RV function compared with PTB rats with compensated RV failure despite similar RV pressures (Q). RVSP: right ventricular systolic pressure; CI: cardiac index. Results are presented as mean with 95% CI. *$p < 0.05$, ***$p < 0.001$ vs sham; †$p < 0.05$, ††$p < 0.01$ vs SuHx; ‡‡$p < 0.01$ vs PTB-comp.

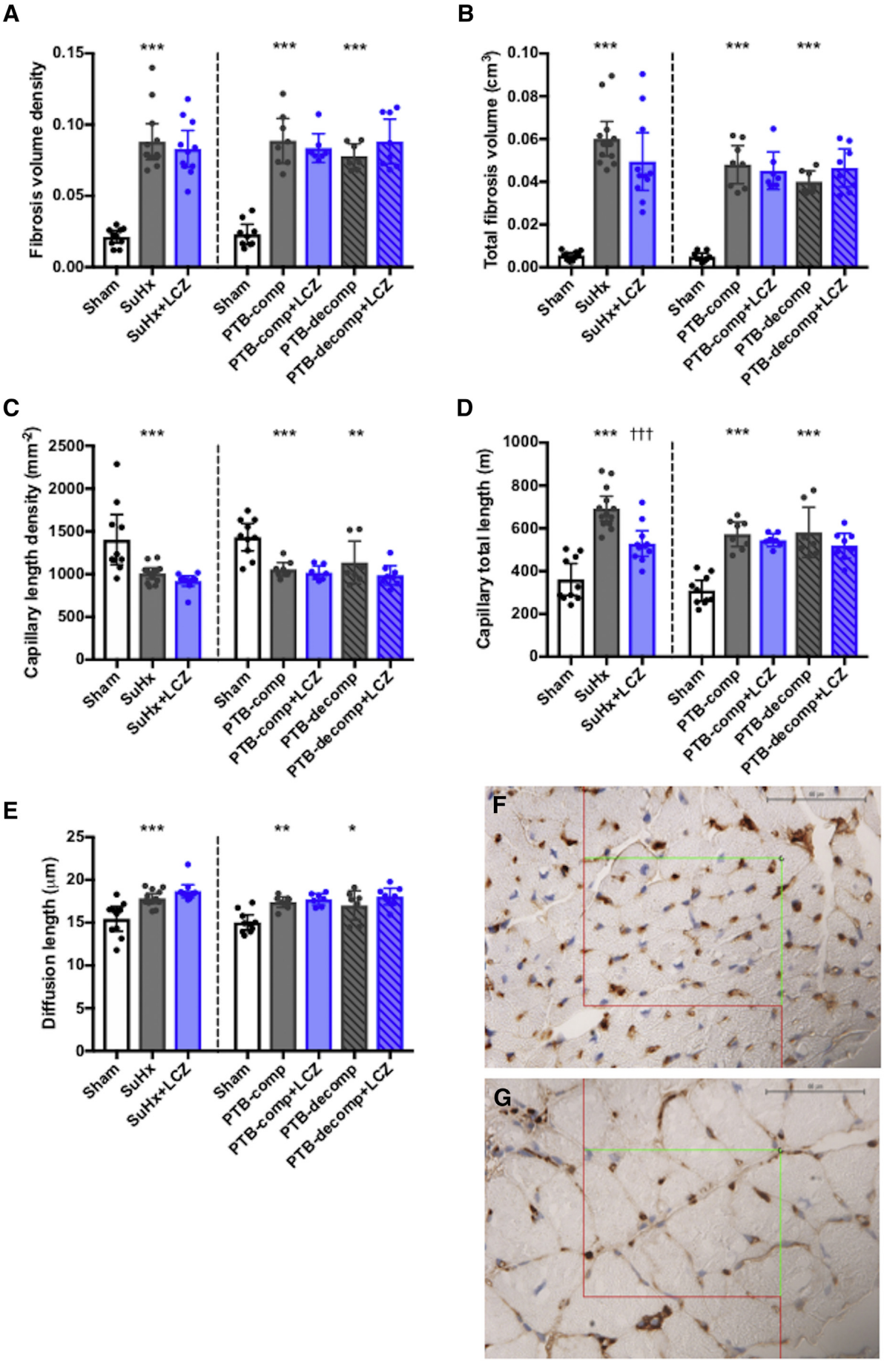
A
Fibrosis volume density
0.15
0.10
0.05
0.00
***
***
***
Sham
SuHx
SuHx+LCZ
Sham
PTB-comp
PTB-comp+LCZ
PTB-decomp
PTB-decomp+LCZ
B
Total fibrosis volume (cm³)
0.10
0.08
0.06
0.04
0.02
0.00
***
***
***
Sham
SuHx
SuHx+LCZ
Sham
PTB-comp
PTB-comp+LCZ
PTB-decomp
PTB-decomp+LCZ
C
Capillary length density (mm⁻²)
2500
2000
1500
1000
500
0
***
***
**
Sham
SuHx
SuHx+LCZ
Sham
PTB-comp
PTB-comp+LCZ
PTB-decomp
PTB-decomp+LCZ
D
Capillary total length (m)
1000
800
600
400
200
0
*** †††
***
***
Sham
SuHx
SuHx+LCZ
Sham
PTB-comp
PTB-comp+LCZ
PTB-decomp
PTB-decomp+LCZ
E
Diffusion length (μm)
25
20
15
10
5
0
***
**
*
Sham
SuHx
SuHx+LCZ
Sham
PTB-comp
PTB-comp+LCZ
PTB-decomp
PTB-decomp+LCZ
F
G

hypoxia [20]. In the monocrotaline model, losartan improved RV function by afterload reduction associated with reduced pulmonary vascular remodeling [2]. Together, these studies suggest a role of angiotensin II in pulmonary vascular remodeling in experimental PH and RV failure. Results from studies investigating the effects of RAAS inhibition in isolated RV failure are contradictory [21,22]. In a previous study, we found no beneficial effects of treatment with the angiotensin II receptor blocker losartan in the PTB model using a losartan dosage comparable to the valsartan dosage of the current study [23].

We observed a minor reduction in systemic blood pressure in both the SuHx and the PTB model comparable to what has been reported previously with a similar dosage of LCZ696 in rats with myocardial infarction [24]. Three out of fourteen rats died before end of study in the LCZ696 treated SuHx group, whereas only one out of fourteen rats died before end of study in the vehicle treated SuHx group. All four rats died suddenly. Although, this difference was not significant, we cannot exclude that the additional deaths in the SuHx+LCZ group were due to disproportional effects of LCZ696 on systemic blood pressure. LCZ696 reduced systemic blood pressure by approximately 12% in the SuHx rats, which is comparable to the systemic blood pressure reduction reported in other studies evaluating blood pressure lowering pharmaceuticals in different RV failure models [2,21,23].

4.2. Pulmonary vascular effects of LCZ696

Using stereological principles and methods, we observed a reduction in pulmonary vascular remodeling. In previous studies, BNP reduced angiotensin II induced pulmonary arterial smooth muscle cell (PA-SMC) proliferation [4], and angiotensin II increased proliferation rate more in PA-SMCs from idiopathic PAH patients compared with PA-SMCs from controls. Co-incubation with the angiotensin II receptor blocker losartan abolished this enhanced response in the idiopathic PAH PA-SMCs, indicating that blockade of the angiotensin II receptor may reduce PA-SMC proliferation in PAH [2].

LCZ696 also works as a vasodilator by inhibiting the phospholipase C mediated vasoconstricting effects of angiotensin II [25] and by enhancing ANP and BNP activation of the particulate guanylyl cyclase to increase cGMP production [26]. In addition, BNP increases NO production [27]. It is therefore most likely that LCZ696 works in the SuHx model by attenuating pulmonary vascular remodeling as well as by pulmonary vasodilation, as also suggested by others [16].

BNP infusions induce pulmonary vasodilation in patients with PH due to left heart disease [6,7,28], but the potential effects of LCZ696 on pulmonary vascular tone and remodeling in this patient group remains to be clarified.

4.3. RV angiogenesis

The question of angiogenesis vs capillary rarefaction in the pressure overloaded RV remains debated. A decrease in capillary density has been reported in different RV failure models [23,29,30], and it has been hypothesized that this reduction is caused by a loss of capillaries [29]. With design-based stereology, it is possible to link unbiased estimates of capillary length density with tissue volumes and thereby obtain an estimate of the total length of the capillaries in the RV. Using stereology, we show a net increase in total capillary length in both the SuHx and the PTB model, although the angiogenic response was not sufficient to prevent an increase in diffusion length (radius of the tissue supplied by a capillary) with RV hypertrophy. These results are in concordance with recent studies in experimental PH [31] and human PAH [32]. Although the absolute increase in diffusion length is minor, it might carry physiological consequences for example during exercise.

4.4. Strengths and limitations

This study has several strengths. First, we used two different animal models of RV failure as recently recommended [33], which allowed us to distinguish pulmonary vascular effects from direct cardiac effects of LCZ696 treatment. Besides providing information on the mechanisms of action of LCZ696, addition of the PTB model enabled us to reject adverse effects of LCZ696 on the RV, which might be masked in the SuHx model due to the beneficial effects of LCZ696 on the pulmonary circulation. We used stereology for an unbiased assessment of the pulmonary vasculature and RV myocardium as recommended for both lungs and the RV [33,34].

However, the study also has some limitations. First of all, neither the SuHx model nor the PTB model resembles human PAH and RV failure completely. Along with interspecies differences between humans and rats, this might limit the translation of our findings. In order to eliminate possible effects of hormonal changes and minimize the physiological variance between the rats, we only used male rats in the study. Besides, we used Sprague-Dawley rats for the SuHx model and Wistar rats for the PTB model as both models are well-established and well-characterized [10,11], and disease development in the two models in these particular rat strains was considered appropriate for evaluation of the effects of LCZ696 on RV failure with and without PH. The use of two different rat strains, however, precludes direct comparison between the two models. Moreover, the mechanisms of disease development differ between the two models, which further complicates comparison of disease severity between the models. However, as the SuHx rats and the PTB-comp rats did not develop extracardiac manifestations of decompensated RV failure (hydrothorax/ascites and nutmeg liver), whereas the PTB-decomp rats did, we believe that the disease stage of the SuHx rats is more comparable to the disease stage of the PTB-comp rats than the PTB-decomp rats. Evaluation of hemodynamics was performed in anaesthetized rats. A well-tested protocol of anesthesia was strictly followed for all rats to minimize the influence of the anesthesia on the measurements. Paraffin tissue sections shrink to a high degree, but this was checked and found to be similar in the various groups.

No pure sacubitril or valsartan group was included in this study, and our results therefore confine to the combination treatment with LCZ696. However, taking the synergistic effects of dual blockade of the angiotensin II receptor and neprilysin [24] into account, LCZ696 represents a distinctive pharmacological treatment. Additionally, a number of studies investigating the effects of isolated blockade of the angiotensin II receptor or isolated stimulation of the natriuretic peptide system in PH and RV failure already exist [2,15–17,20–23].

In conclusion, combined angiotensin II receptor antagonism and neprilysin inhibition by long-term treatment with LCZ696 reduced RV systolic pressure, hypertrophy, and dilatation in the SuHx model of PH and RV failure. In the PTB model of isolated RV failure, LCZ696 treatment did not demonstrate similar effects indicating that the beneficial effects seen in the SuHx model may be attributed to pulmonary vascular effects rather than direct cardiac effects. In both models, LCZ696 was well-tolerated. Despite the absence of direct beneficial effects of LCZ696 on RV function in this study, future studies should address the therapeutic potential of combined angiotensin II receptor antagonism and neprilysin inhibition in different groups of PH patients.

Fig. 3. RV remodeling in the SuHx and the PTB model. The volume fraction of RV fibrosis (A) as well as the total volume of RV fibrosis (B) were increased in both SuHx and PTB rats compared with sham. Capillary length density was decreased in SuHx and PTB rats compared with sham rats (C), although an increase in total length of the capillaries revealed that angiogenesis accompanies the hypertrophy of the pressure overloaded RV (D). The angiogenic response was, however, not sufficient to prevent an increase in diffusion length (E). Representative images of RV tissue stained with CD31 antibodies for visualization of capillaries with a superimposed unbiased counting frame from a sham rat (F) and a PTB-comp rat (G). Data are presented as mean with 95% CI. $^{*}p < 0.05$, $^{**}p < 0.01$, $^{***}p < 0.001$ vs sham; $^{\dagger\dagger\dagger}p < 0.001$ vs SuHx.

Grant support

This work was supported by Aarhus University, Denmark to S.A.; the Danish Heart Foundation [16-R107-A6611-22969 to S.A.]; Fonden til Lægevidenskabens Fremme – The A.P. Møller Foundation to S.A.; Villum Foundation to J.R.N. and Novo Nordic Foundation [NNF17OC0024868 to J.E.N.-K. and A.A.]. This work was further supported by the Netherlands CardioVascular Research Initiative; the Dutch Heart Foundation; Dutch Federation of University Medical Centres; the Netherlands Organization for Health Research and Development and the Royal Netherlands Academy of Sciences to H.J.B. and F.d.M.

Declaration of Competing Interest

The authors report no relationships that could be construed as a conflict of interest.

Acknowledgements

The author thanks Helene Andersen, Core Center for Molecular Morphology, Section for Stereology and Microscopy, Aarhus University for much appreciated technical assistance and help with preparation of tissue sections for stereological analyses.

Appendix A. Supplementary data

Supplementary data to this article can be found online at https://doi.org/10.1016/j.ijcard.2019.06.065.

References

[1] C. Orte, J.M. Polak, S.G. Haworth, M.H. Yacoub, N.W. Morrell, Expression of pulmonary vascular angiotensin-converting enzyme in primary and secondary plexiform pulmonary hypertension, J. Pathol. 192 (3) (2000) 379–384.
[2] F.S. de Man, L. Tu, M.L. Handoko, S. Rain, G. Ruiter, C. François, et al., Dysregulated renin-angiotensin-aldosterone system contributes to pulmonary arterial hypertension, Am. J. Respir. Crit. Care Med. 186 (8) (2012) 780–789.
[3] A.A. Arjona, C.A. Hsu, D.S. Wrenn, N.S. Hill, Effects of natriuretic peptides on vascular smooth-muscle cells derived from different vascular beds, Gen. Pharmacol. 28 (3) (1997) 387–392.
[4] J.H. Hsu, S.F. Liou, S.N. Yang, B.N. Wu, Z.K. Dai, I.J. Chen, et al., B-type natriuretic peptide inhibits angiotensin II-induced proliferation and migration of pulmonary arterial smooth muscle cells, Pediatr. Pulmonol. 49 (8) (2014) 734–744.
[5] L. Zhao, L. Long, N.W. Morrell, M.R. Wilkins, NPR-A-deficient mice show increased susceptibility to hypoxia-induced pulmonary hypertension, Circulation. 99 (5) (1999) 605–607.
[6] A.D. Michaels, K. Chatterjee, T. De Marco, Effects of intravenous nesiritide on pulmonary vascular hemodynamics in pulmonary hypertension, J. Card. Fail. 11 (6) (2005) 425–431.
[7] K.K. Khush, T. De Marco, K.T. Vakharia, C. Harmon, J.R. Fineman, K. Chatterjee, et al., Nesiritide acutely increases pulmonary and systemic levels of nitric oxide in patients with pulmonary hypertension, J. Card. Fail. 12 (7) (2006) 507–513.
[8] J.R. Klinger, S. Thaker, J. Houtchens, I.R. Preston, N.S. Hill, H.W. Farber, Pulmonary hemodynamic responses to brain natriuretic peptide and sildenafil in patients with pulmonary arterial hypertension, Chest. 129 (2) (2006) 417–425.
[9] J.J.V. McMurray, M. Packer, A.S. Desai, J. Gong, M.P. Lefkowitz, A.R. Rizkala, et al., Angiotensin-neprilysin inhibition versus enalapril in heart failure, N. Engl. J. Med. 371 (11) (2014) 993–1004.
[10] M.A. de Raaf, I. Schalij, J. Gomez-Arroyo, N. Rol, C. Happé, F.S. de Man, et al., SuHx rat model: partly reversible pulmonary hypertension and progressive intima obstruction, Eur. Respir. J. 44 (1) (2014) 160–168.
[11] S. Andersen, J. Schultz, S. Holmboe, J. Axelsen, M. Hansen, M. Lyhne, et al., A pulmonary trunk banding model of pressure overload induced right ventricular hypertrophy and failure, J. Vis. Exp. (141) (2018).
[12] J.R. Nyengaard, H.J. Gundersen, Sampling for stereology in lungs, Eur. Respir. Rev. 15 (101) (2006) 107–114.
[13] J.R. Nyengaard, The isector: a simple and direct method for generating isotropic, uniform random sections from small specimens, J. Microsc. 165 (1992) 427–431.
[14] A. Bruel, H. Oxlund, J.R. Nyengaard, Growth hormone increases the total number of myocyte nuclei in the left ventricle of adult rats, Growth Hormon. IGF Res. 12 (2) (2002) 106–115.
[15] R.J. Winter, L. Zhao, T. Krausz, J.M. Hughes, Neutral endopeptidase 24.11 inhibition reduces pulmonary vascular remodeling in rats exposed to chronic hypoxia, Am. Rev. Respir. Dis. 144 (6) (1991) 1342–1346.
[16] J.R. Klinger, R.R. Warburton, L. Pietras, N.S. Hill, Brain natriuretic peptide inhibits hypoxic pulmonary hypertension in rats, J. Appl. Physiol. 84 (5) (1998) 1646–1652.
[17] C. Carlino, J.D. Tobias, R.I. Schneider, R.L. Heller, M.A. Alpert, R.E. Grueber, et al., Pulmonary hemodynamic response to acute combination and monotherapy with sildenafil and brain natriuretic peptide in rats with monocrotaline-induced pulmonary hypertension, Am J Med Sci 339 (1) (2009) 55–59.
[18] N.W. Morrell, E.N. Atochina, K.G. Morris, S.M. Danilov, K.R. Stenmark, Angiotensin converting enzyme expression is increased in small pulmonary arteries of rats with hypoxia-induced pulmonary hypertension, J. Clin. Invest. 96 (4) (1995) 1823–1833.
[19] N.W. Morrell, S.M. Danilov, K.B. Satyan, K.G. Morris, K.R. Stenmark, Right ventricular angiotensin converting enzyme activity and expression is increased during hypoxic pulmonary hypertension, Cardiovasc. Res. 34 (2) (1997) 393–403.
[20] N.W. Morrell, K.G. Morris, K.R. Stenmark, Role of angiotensin-converting enzyme and angiotensin II in development of hypoxic pulmonary hypertension, Am. J. Phys. 269 (4 Pt 2) (1995) H1186–H1194.
[21] M.A. Borgdorff, B. Bartelds, M.G. Dickinson, P. Steendijk, R.M.F. Berger, A cornerstone of heart failure treatment is not effective in experimental right ventricular failure, Int. J. Cardiol. 169 (3) (2013) 183–189.
[22] M.K. Friedberg, M.-Y. Cho, J. Li, R.S. Assad, M. Sun, S. Rohailla, et al., Adverse biventricular remodeling in isolated right ventricular hypertension is mediated by increased transforming growth factor-β1 signaling and is abrogated by angiotensin receptor blockade, Am. J. Respir. Cell Mol. Biol. 49 (6) (2013) 1019–1028.
[23] S. Andersen, J.G. Schultz, A. Andersen, S. Ringgaard, J.M. Nielsen, S. Holmboe, et al., Effects of bisoprolol and losartan treatment in the hypertrophic and failing right heart, J. Card. Fail. 20 (11) (2014) 864–873.
[24] T.G. von Lueder, B.H. Wang, A.R. Kompa, L. Huang, R. Webb, P. Jordaan, et al., Angiotensin receptor neprilysin inhibitor LCZ696 attenuates cardiac remodeling and dysfunction after myocardial infarction by reducing cardiac fibrosis and hypertrophy, Circ. Heart Fail. 8 (1) (2014) 71–78.
[25] M. Paul, A. Poyan Mehr, R. Kreutz, Physiology of local renin-angiotensin systems, Physiol. Rev. 86 (3) (2006) 747–803.
[26] A. Buglioni, J.C. Burnett, New pharmacological strategies to increase cGMP, Annu. Rev. Med. 67 (2015) 229–243.
[27] K. van der Zander, A.J. Houben, A.A. Kroon, J.G. De Mey, P.A. Smits, P.W. de Leeuw, Nitric oxide and potassium channels are involved in brain natriuretic peptide induced vasodilatation in man, J. Hypertens. 20 (3) (2002) 493–499.
[28] T. Chen, N. Jiang, L. Wang, Z. Guo, J. Han, S. Jing, et al., The significance of natriuretic peptide in treatment of pulmonary hypertension after mitral valve replacement, J. Thorac. Cardiovasc. Surg. 147 (4) (2013) 1362–1367.
[29] H.J. Bogaard, R. Natarajan, S.C. Henderson, C.S. Long, D. Kraskauskas, L. Smithson, et al., Chronic pulmonary artery pressure elevation is insufficient to explain right heart failure, Circulation. 120 (20) (2009) 1951–1960.
[30] H.J. Bogaard, R. Natarajan, S. Mizuno, A. Abbate, P.J. Chang, V.Q. Chau, et al., Adrenergic receptor blockade reverses right heart remodeling and dysfunction in pulmonary hypertensive rats, Am. J. Respir. Crit. Care Med. 182 (5) (2010) 652–660.
[31] B.B. Graham, R. Kumar, C. Mickael, B. Kassa, D. Koyanagi, L. Sanders, et al., Vascular adaptation of the right ventricle in experimental pulmonary hypertension, Am. J. Respir. Cell Mol. Biol. 59 (2018) 479–489.
[32] B.B. Graham, D. Koyanagi, B. Kandasamy, R.M. Tuder, Right ventricle vasculature in human pulmonary hypertension assessed by stereology, Am. J. Respir. Crit. Care Med. 196 (2017) 1075–1077.
[33] T. Lahm, I.S. Douglas, S.L. Archer, H.J. Bogaard, N.C. Chesler, F. Haddad, et al., Assessment of right ventricular function in the research setting: knowledge gaps and pathways forward. An official American Thoracic Society research statement, Am. J. Respir. Crit. Care Med. 198 (4) (2018) e15–e43.
[34] C.C. Hsia, D.M. Hyde, M. Ochs, E.R. Weibel, An official research policy statement of the American Thoracic Society/European Respiratory Society: standards for quantitative assessment of lung structure, Am. J. Respir. Crit. Care Med. 181 (4) (2010) 394–418.